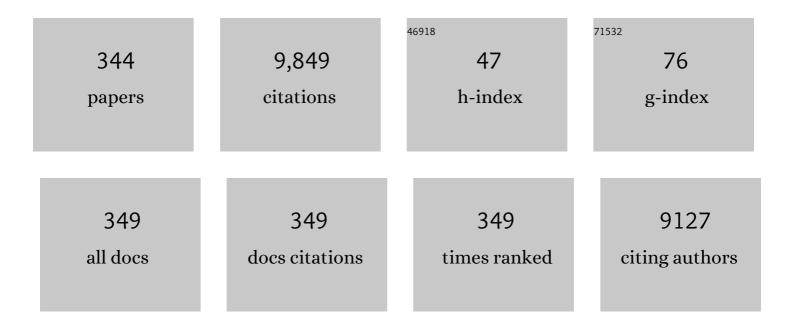
List of Publications by Year in descending order

Source: https://exaly.com/author-pdf/9090908/publications.pdf Version: 2024-02-01



#	Article	IF	CITATIONS
1	Pressure-induced metallization of dense (H2S)2H2 with high-Tc superconductivity. Scientific Reports, 2014, 4, 6968.	1.6	802
2	Pressure-induced decomposition of solid hydrogen sulfide. Physical Review B, 2015, 91, .	1.1	255
3	Long-Range Ordered Carbon Clusters: A Crystalline Material with Amorphous Building Blocks. Science, 2012, 337, 825-828.	6.0	173
4	Facile fabrication of faceted copper nanocrystals with high catalytic activity for p-nitrophenol reduction. Journal of Materials Chemistry A, 2013, 1, 1632-1638.	5.2	157
5	Luminescence Properties of Compressed Tetraphenylethene: The Role of Intermolecular Interactions. Journal of Physical Chemistry Letters, 2014, 5, 2968-2973.	2.1	154
6	Facile synthesis of iv–vi SnS nanocrystals with shape and size control: Nanoparticles, nanoflowers and amorphous nanosheets. Nanoscale, 2010, 2, 1699.	2.8	119
7	Highly Enhanced Luminescence from Single-Crystalline C60·1m-xylene Nanorods. Chemistry of Materials, 2006, 18, 4190-4194.	3.2	117
8	Facile Synthesis of Tin Oxide Nanoflowers: A Potential High-Capacity Lithium-Ion-Storage Material. Langmuir, 2009, 25, 1818-1821.	1.6	109
9	Structure and superconductivity of hydrides at high pressures. National Science Review, 2017, 4, 121-135.	4.6	109
10	Syntheses, Characterizations, and Applications in Lithium Ion Batteries of Hierarchical SnO Nanocrystals. Journal of Physical Chemistry C, 2009, 113, 14140-14144.	1.5	105
11	Superconducting high-pressure phases of disilane. Proceedings of the National Academy of Sciences of the United States of America, 2010, 107, 9969-9973.	3.3	102
12	Single-Molecule Force Spectroscopy on Poly(acrylic acid) by AFM. Langmuir, 1999, 15, 2120-2124.	1.6	100
13	Size-Dependent Amorphization of Nanoscale <mml:math xmlns:mml="http://www.w3.org/1998/Math/MathML" display="inline"><mml:msub><mml:mi mathvariant="bold">Y<mml:mn>2</mml:mn></mml:mi </mml:msub><mml:msub><mml:msub><mml:mi mathvariant="bold">O<mml:mn>3</mml:mn></mml:mi </mml:msub></mml:msub></mml:math 	2.9	100
14	display="inline"> <mml:mrow><mml:mi>s</mml:mi><mml:msup><mml:mi>p</mml:mi><mml:mi>3<!--<br-->Carbon Allotrope from Cold-Compressed <mml:math xmlns:mml="http://www.w3.org/1998/Math/MathML" display="inline"><mml:mrow><mml:msub><mml:mi mathvariant="normal">C</mml:mi </mml:msub></mml:mrow></mml:math </mml:mi><mml:mrow><mml:mn>70</mml:mn></mml:mrow></mml:msup></mml:mrow> <td>2.9</td> <td>100</td>	2.9	100
15	Peapods. Physical Review Letters, 2017, 118, 245701. Ultrahard bulk amorphous carbon from collapsed fullerene. Nature, 2021, 599, 599-604.	13.7	99
16	Controlled Synthesis of Hollow Cu _{2â€x} Te Nanocrystals Based on the Kirkendall Effect and Their Enhanced CO Gas‣ensing Properties. Small, 2013, 9, 793-799.	5.2	94
17	A one-step green route to synthesize copper nanocrystals and their applications in catalysis and surface enhanced Raman scattering. Nanoscale, 2014, 6, 5343.	2.8	83
18	Lowest enthalpy polymorph of cold-compressed graphite phase. Physical Chemistry Chemical Physics, 2012, 14, 4347.	1.3	80

#	Article	IF	CITATIONS
19	Raman signature to identify the structural transition of single-wall carbon nanotubes under high pressure. Physical Review B, 2008, 78, .	1.1	79
20	<i>Ab initio</i> study revealing a layered structure in hydrogen-rich KH <mml:math xmlns:mml="http://www.w3.org/1998/Math/MathML" display="inline"><mml:msub><mml:mrow /><mml:mn>6</mml:mn></mml:mrow </mml:msub>under high pressure. Physical Review B, 2012, 86, .</mml:math 	1.1	79
21	Alkaline-earth metal (Mg) polynitrides at high pressure as possible high-energy materials. Physical Chemistry Chemical Physics, 2017, 19, 9246-9252.	1.3	77
22	Synthesis and growth mechanism of differently shaped C60 nano/microcrystals produced by evaporation of various aromatic C60 solutions. Carbon, 2009, 47, 1181-1188.	5.4	76
23	Recent advances in IV–VI semiconductor nanocrystals: synthesis, mechanism, and applications. RSC Advances, 2013, 3, 8104.	1.7	76
24	Improved Lithiumâ€Ion and Sodiumâ€Ion Storage Properties from Fewâ€Layered WS ₂ Nanosheets Embedded in a Mesoporous CMKâ€3 Matrix. Chemistry - A European Journal, 2017, 23, 7074-7080.	1.7	75
25	Competition between insertion of Li + and Mg 2+ : An example of TiO 2 -B nanowires for Mg rechargeable batteries and Li + /Mg 2+ hybrid-ion batteries. Journal of Power Sources, 2017, 346, 134-142.	4.0	70
26	Synthesis and Mechanism of Particle- and Flower-Shaped ZnSe Nanocrystals: Green Chemical Approaches toward Green Nanoproducts. Journal of Physical Chemistry C, 2008, 112, 7567-7571.	1.5	69
27	Pressure-Induced Amorphization and Polyamorphism in One-Dimensional Single-Crystal TiO ₂ Nanomaterials. Journal of Physical Chemistry Letters, 2010, 1, 309-314.	2.1	68
28	Shape and size controlled synthesis and properties of colloidal IV–VI SnSe nanocrystals. CrystEngComm, 2011, 13, 4161.	1.3	68
29	A Novel Polymerization of Nitrogen in Beryllium Tetranitride at High Pressure. Journal of Physical Chemistry C, 2017, 121, 9766-9772.	1.5	67
30	High-temperature superconductivity in sulfur hydride evidenced by alternating-current magnetic susceptibility. National Science Review, 2019, 6, 713-718.	4.6	63
31	Synthesis of High-Density Nanocavities inside TiO ₂ â^B Nanoribbons and Their Enhanced Electrochemical Lithium Storage Properties. Inorganic Chemistry, 2008, 47, 9870-9873.	1.9	62
32	Hydrothermal synthesis of \hat{I}^3 -MnOOH nanorods and their conversion to MnO2, Mn2O3, and Mn3O4 nanorods. Journal of Alloys and Compounds, 2015, 644, 430-437.	2.8	62
33	Nitrogen concentration driving the hardness of rhenium nitrides. Scientific Reports, 2014, 4, 4797.	1.6	61
34	Superhard three-dimensional carbon with metallic conductivity. Carbon, 2017, 123, 311-317.	5.4	61
35	Superhard semiconductingC3N2compounds predicted via first-principles calculations. Physical Review B, 2008, 78, .	1.1	60
36	Structural stability of polymeric nitrogen: A first-principles investigation. Journal of Chemical Physics, 2010, 132, 024502.	1.2	60

#	Article	IF	CITATIONS
37	One-step solution synthesis of bismuth sulfide (Bi ₂ S ₃) with various hierarchical architectures and their photoresponse properties. RSC Advances, 2012, 2, 234-240.	1.7	59
38	Divergent synthesis routes and superconductivity of ternary hydride <mml:math xmlns:mml="http://www.w3.org/1998/Math/MathML"><mml:msub><mml:mi>MgSiH</mml:mi><mml:mn>6high pressure. Physical Review B, 2017, 96, .</mml:mn></mml:msub></mml:math 	nml :1 010> </td <td>mmtansub></td>	mm ta nsub>
39	Synthesis of polyhedron hollow structure Cu2O and their gas-sensing properties. Sensors and Actuators B: Chemical, 2012, 171-172, 135-140.	4.0	56
40	lsolation of Three Isomers of Sm@C ₈₄ and X-ray Crystallographic Characterization of Sm@ <i>D</i> _{3<i>d</i>} (19)-C ₈₄ and Sm@ <i>C</i> ₂ (13)-C ₈₄ . Journal of the American Chemical Society, 2012, 134, 5331-5338.	6.6	55
41	Mechanical and metallic properties of tantalum nitrides from first-principles calculations. RSC Advances, 2014, 4, 10133.	1.7	55
42	Stability of Hydrogen-Bonded Supramolecular Architecture under High Pressure Conditions: Pressure-Induced Amorphization in Melamineâ^'Boric Acid Adduct. Langmuir, 2009, 25, 4787-4791.	1.6	54
43	Solution synthesis of copper selenide nanocrystals and their electrical transport properties. CrystEngComm, 2012, 14, 2139.	1.3	54
44	Temperature dependence of band gap in CdSe nanocrystals. Chemical Physics Letters, 2007, 439, 65-68.	1.2	52
45	Pressure-Induced Phase Transition in Hydrogen-Bonded Supramolecular Adduct Formed by Cyanuric Acid and Melamine. Journal of Physical Chemistry B, 2009, 113, 14719-14724.	1.2	52
46	Two-dimensional Penta-BP5 Sheets: High-stability, Strain-tunable Electronic Structure and Excellent Mechanical Properties. Scientific Reports, 2017, 7, 2404.	1.6	52
47	Pressure-Induced Phase Transition in N–H···O Hydrogen-Bonded Molecular Crystal Oxamide. Journal of Physical Chemistry B, 2012, 116, 9796-9802.	1.2	49
48	Single molecule force spectroscopy on poly(vinyl alcohol) by atomic force microscopy. Macromolecular Rapid Communications, 1998, 19, 609-612.	2.0	48
49	Polymorphism and Formation Mechanism of Nanobipods in Manganese Sulfide Nanocrystals Induced by Temperature or Pressure. Journal of Physical Chemistry C, 2012, 116, 3292-3297.	1.5	48
50	Pressure-induced SERS enhancement in a MoS ₂ /Au/R6G system by a two-step charge transfer process. Nanoscale, 2019, 11, 21493-21501.	2.8	48
51	Cubic C ₉₆ : a novel carbon allotrope with a porous nanocube network. Journal of Materials Chemistry A, 2015, 3, 10448-10452.	5.2	47
52	Orthorhombic C14 carbon: A novel superhard sp3 carbon allotrope. Carbon, 2020, 156, 309-312.	5.4	47
53	Hexagonal-structured ε-NbN: ultra-incompressibility, high shear rigidity and a possible hard superconducting material. Scientific Reports, 2015, 5, 10811.	1.6	46
54	Synthesis and characterization of single-walled nanotubes produced with Ce/Ni as catalysts. Chemical Physics Letters, 2000, 320, 365-372.	1.2	45

#	Article	IF	CITATIONS
55	Morphology-Tuned Phase Transitions of Anatase TiO ₂ Nanowires under High Pressure. Journal of Physical Chemistry C, 2013, 117, 8516-8521.	1.5	45
56	Exploration of the Pyrazinamide Polymorphism at High Pressure. Journal of Physical Chemistry B, 2012, 116, 14441-14450.	1.2	44
57	High pressure transformation of graphene nanoplates: A Raman study. Chemical Physics Letters, 2013, 585, 101-106.	1.2	44
58	Low-temperature synthesis of porous hollow structured Cu2O for photocatalytic activity and gas sensor application. RSC Advances, 2013, 3, 18651.	1.7	44
59	Synthesis and high pressure induced amorphization of C60 nanosheets. Applied Physics Letters, 2007, 91, .	1.5	43
60	Rotational dynamics of confined C ₆₀ from near-infrared Raman studies under high pressure. Proceedings of the National Academy of Sciences of the United States of America, 2009, 106, 22135-22138.	3.3	43
61	Selfâ€Assembled CoS Nanoflowers Wrapped in Reduced Graphene Oxides as the Highâ€Performance Anode Materials for Sodiumâ€ion Batteries. Chemistry - A European Journal, 2017, 23, 13150-13157.	1.7	43
62	Synthesis of narrow band gap SnTe nanocrystals: nanoparticles and single crystal nanowires via oriented attachment. CrystEngComm, 2010, 12, 4275.	1.3	42
63	Ultrathin TiO ₂ -B nanowires as an anode material for Mg-ion batteries based on a surface Mg storage mechanism. Nanoscale, 2017, 9, 12934-12940.	2.8	42
64	Hydrogen bond symmetrization and superconducting phase of HBr and HCl under high pressure: An <i>ab initio</i> study. Journal of Chemical Physics, 2010, 133, 074509.	1.2	41
65	Decompression-Induced Diamond Formation from Graphite Sheared under Pressure. Physical Review Letters, 2020, 124, 065701.	2.9	41
66	Molecular insertion regulates the donor-acceptor interactions in cocrystals for the design of piezochromic luminescent materials. Nature Communications, 2021, 12, 4084.	5.8	41
67	Cubic gauche-CN: A superhard metallic compound predicted via first-principles calculations. Journal of Chemical Physics, 2010, 133, 044512.	1.2	40
68	Prediction of superconducting ternary hydride MgGeH ₆ : from divergent high-pressure formation routes. Physical Chemistry Chemical Physics, 2017, 19, 27406-27412.	1.3	40
69	Pressure-Induced Irreversible Phase Transition in the Energetic Material Urea Nitrate: Combined Raman Scattering and X-ray Diffraction Study. Journal of Physical Chemistry C, 2013, 117, 152-159.	1.5	39
70	Pressure-Induced Phase Transition in N–H···O Hydrogen-Bonded Molecular Crystal Biurea: Combined Raman Scattering and X-ray Diffraction Study. Journal of Physical Chemistry C, 2014, 118, 15162-15168.	1.5	39
71	Synthesis and high-pressure transformation of metastable wurtzite-structured CuGaS2 nanocrystals. Nanoscale, 2012, 4, 7443.	2.8	38
72	Ternary superconducting cophosphorus hydrides stabilized via lithium. Npj Computational Materials, 2019, 5, .	3.5	38

#	Article	IF	CITATIONS
73	Colloidal CdSe Nanocrystals Synthesized in Noncoordinating Solvents with the Addition of a Secondary Ligand:Â Exceptional Growth Kinetics. Journal of Physical Chemistry B, 2006, 110, 16508-16513.	1.2	37
74	Ethylene glycol-mediated synthesis of nanoporous anatase TiO2 rods and rutile TiO2 self-assembly chrysanthemums. Journal of Alloys and Compounds, 2009, 471, 477-480.	2.8	36
75	Facile synthesis of hydrogenated carbon nanospheres with a graphite-like ordered carbon structure. Nanoscale, 2013, 5, 11306.	2.8	36
76	Exploration of the Hydrogen-Bonded Energetic Material Carbohydrazide at High Pressures. Journal of Physical Chemistry C, 2014, 118, 22960-22967.	1.5	36
77	Discovery of Superconductivity in Hard Hexagonal ε-NbN. Scientific Reports, 2016, 6, 22330.	1.6	36
78	Significantly narrowed bandgap and enhanced charge separation in porous, nitrogen-vacancy red g-C3N4 for visible light photocatalytic H2 production. Applied Surface Science, 2020, 504, 144407.	3.1	36
79	New High Pressure Phases of the Zn–N System. Journal of Physical Chemistry C, 2020, 124, 4044-4049.	1.5	36
80	<i>Ab initio</i> studies of solid bromine under high pressure. Physical Review B, 2007, 76, .	1.1	35
81	Size-Controlled Synthesis of Bifunctional Magnetic and Ultraviolet Optical Rock-Salt MnS Nanocube Superlattices. Langmuir, 2012, 28, 17811-17816.	1.6	35
82	Synthesis of single-wall carbon nanotubes and long nanotube ribbons with Ho/Ni as catalyst by arc discharge. Carbon, 2005, 43, 2894-2901.	5.4	34
83	High-Pressure Studies on CeO ₂ Nano-Octahedrons with a (111)-Terminated Surface. Journal of Physical Chemistry C, 2011, 115, 4546-4551.	1.5	34
84	Synthesis of differently shaped C70 nano/microcrystals by using various aromatic solvents and their crystallinity-dependent photoluminescence. Carbon, 2012, 50, 209-215.	5.4	34
85	Transparent, superhard amorphous carbon phase from compressing glassy carbon. Applied Physics Letters, 2014, 104, 021916.	1.5	34
86	Tailoring Building Blocks and Their Boundary Interaction for the Creation of New, Potentially Superhard, Carbon Materials. Advanced Materials, 2015, 27, 3962-3968.	11.1	34
87	Pressure-Induced Structures and Properties in Indium Hydrides. Inorganic Chemistry, 2015, 54, 9924-9928.	1.9	34
88	Bonding Properties of Aluminum Nitride at High Pressure. Inorganic Chemistry, 2017, 56, 7494-7500.	1.9	34
89	Facile synthesis of magic-sized CdSe and CdTe nanocrystals with tunable existence periods. Nanotechnology, 2007, 18, 405603.	1.3	33
90	Pressure-Induced Phase Transition in Hydrogen-Bonded Supramolecular Structure: Guanidinium Nitrate. Journal of Physical Chemistry B, 2010, 114, 6765-6769.	1.2	33

#	Article	IF	CITATIONS
91	Reversible Polymerization in Doped Fullerides Under Pressure: The Case Of C ₆₀ (Fe(C ₅ H ₅) ₂) ₂ . Journal of Physical Chemistry B, 2012, 116, 2643-2650.	1.2	33
92	Unexpected Roomâ€Temperature Ferromagnetism in Nanostructured Bi ₂ Te ₃ . Angewandte Chemie - International Edition, 2014, 53, 729-733.	7.2	33
93	High pressure structures and superconductivity of AlH ₃ (H ₂) predicted by first principles. RSC Advances, 2015, 5, 5096-5101.	1.7	33
94	Potentially superhard hcp <mml:math xmlns:mml="http://www.w3.org/1998/Math/MathML"><mml:mrow><mml:mi>Cr</mml:mi><mml:msub><mml:mi mathvariant="normal">N<mml:mn>2</mml:mn></mml:mi </mml:msub></mml:mrow>compound studied at high pressure. Physical Review B, 2016, 93, .</mml:math 	1.1	33
95	Unique Phase Diagram and Superconductivity of Calcium Hydrides at High Pressures. Inorganic Chemistry, 2019, 58, 2558-2564.	1.9	33
96	Large Volume Collapse during Pressure-Induced Phase Transition in Lithium Amide. Journal of Physical Chemistry C, 2012, 116, 9744-9749.	1.5	32
97	Structural phase transition and photoluminescence properties of YF3 and YF3:Eu3+ under high pressure. Physical Chemistry Chemical Physics, 2013, 15, 19925.	1.3	32
98	Novel Allâ€Nitrogen Molecular Crystals of Aromatic N ₁₀ . Advanced Science, 2020, 7, 1902320.	5.6	32
99	Pressure-Induced Phase Transitions of C ₇₀ Nanotubes. Journal of Physical Chemistry C, 2011, 115, 8918-8922.	1.5	31
100	High-temperature superconductivity in ternary clathrate YCaH ₁₂ under high pressures. Journal of Physics Condensed Matter, 2019, 31, 245404.	0.7	31
101	New Cadmium–Nitrogen Compounds at High Pressures. Inorganic Chemistry, 2021, 60, 6772-6781.	1.9	31
102	A new phase of solid iodine with different molecular covalent bonds. Proceedings of the National Academy of Sciences of the United States of America, 2008, 105, 4999-5001.	3.3	30
103	Pressure-Induced Reversible Phase Transformation in Nanostructured Bi ₂ Te ₃ with Reduced Transition Pressure. Journal of Physical Chemistry C, 2015, 119, 3843-3848.	1.5	30
104	Stability of Sulfur Nitrides: A First-Principles Study. Journal of Physical Chemistry C, 2017, 121, 1515-1520.	1.5	30
105	Pressure-induced transformation and superhard phase in fullerenes: The effect of solvent intercalation. Applied Physics Letters, 2013, 103, .	1.5	29
106	Pressure-induced isosymmetric phase transition in sulfamic acid: A combined Raman and x-ray diffraction study. Journal of Chemical Physics, 2013, 138, 214505.	1.2	29
107	A New Carbon Phase Constructed by Longâ€Range Ordered Carbon Clusters from Compressing C ₇₀ Solvates. Advanced Materials, 2014, 26, 7257-7263.	11.1	29
108	Modulated T carbon-like carbon allotropes: an ab initio study. RSC Advances, 2014, 4, 17364.	1.7	29

#	Article	IF	CITATIONS
109	Structural Phase Transition and Photoluminescence Properties of YF ₃ :Eu ³⁺ Nanocrystals under High Pressure. Journal of Physical Chemistry C, 2014, 118, 22739-22745.	1.5	29
110	High-Pressure-Induced Polymorphic Transformation of Maleic Hydrazide. Journal of Physical Chemistry C, 2014, 118, 8122-8127.	1.5	29
111	Structures and Properties of Osmium Hydrides under Pressure from First Principle Calculation. Journal of Physical Chemistry C, 2015, 119, 15905-15911.	1.5	29
112	Structural phase transition and superconductivity hierarchy in 1T-TaS2 under pressure up to 100 GPa. Npj Quantum Materials, 2021, 6, .	1.8	29
113	Pressure-Induced Phase Transitions in Ammonium Squarate: A Supramolecular Structure Based on Hydrogen-Bonding and π-Stacking Interactions. Journal of Physical Chemistry B, 2011, 115, 8981-8988.	1.2	28
114	The Study of Structural Transition of ZnS Nanorods under High Pressure. Journal of Physical Chemistry C, 2011, 115, 357-361.	1.5	28
115	Direct Zircon-to-Scheelite Structural Transformation in YPO ₄ and YPO ₄ :Eu ³⁺ Nanoparticles Under High Pressure. Journal of Physical Chemistry C, 2012, 116, 24837-24844.	1.5	28
116	Pressure-induced isostructural phase transition of a metal–organic framework Co ₂ (4,4′-bpy) ₃ (NO ₃) ₄ ·xH ₂ O. CrystEngComm, 2014, 16, 4084-4087.	1.3	28
117	Ultrahard boron-rich tantalum boride: Monoclinic TaB 4. Journal of Alloys and Compounds, 2014, 617, 660-664.	2.8	28
118	Raman spectroscopy study of carbon nanotube peapods excited by near-IR laser under high pressure. Physical Review B, 2007, 76, .	1.1	27
119	Effect of High Pressure on the Typical Supramolecular Structure of Guanidinium Methanesulfonate. Journal of Physical Chemistry B, 2012, 116, 3092-3098.	1.2	27
120	Morphology-controlled synthesis of anisotropic wurtzite MnSe nanocrystals: optical and magnetic properties. CrystEngComm, 2012, 14, 6916.	1.3	27
121	Phase diagram, mechanical properties, and electronic structure of Nb–N compounds under pressure. Physical Chemistry Chemical Physics, 2015, 17, 22837-22845.	1.3	27
122	Investigation of charge-transfer between a 4-mercaptobenzoic acid monolayer and TiO ₂ nanoparticles under high pressure using surface-enhanced Raman scattering. Chemical Communications, 2018, 54, 6280-6283.	2.2	27
123	Electric resistance of single-walled carbon nanotubes under hydrostatic pressure. Solid State Communications, 2001, 118, 31-36.	0.9	26
124	Synthesis, optical properties and growth process of In2S3 nanoparticles. Journal of Colloid and Interface Science, 2010, 347, 172-176.	5.0	26
125	A facile approach to PbS nanoflowers and their shape-tunable single crystal hollow nanostructures: Morphology evolution. CrystEngComm, 2011, 13, 199-203.	1.3	26
126	Miscibility and ordered structures of MgO-ZnO alloys under high pressure. Scientific Reports, 2014, 4, 5759.	1.6	26

#	Article	IF	CITATIONS
127	First-principles study on the structural and electronic properties of metallic HfH2 under pressure. Scientific Reports, 2015, 5, 11381.	1.6	26
128	Stability and properties of the Ru–H system at high pressure. Physical Chemistry Chemical Physics, 2016, 18, 1516-1520.	1.3	26
129	Heterostructural MnO ₂ @NiS ₂ /Ni(OH) ₂ materials for high-performance pseudocapacitor electrodes. RSC Advances, 2017, 7, 44289-44295.	1.7	26
130	Structural and dynamical properties of solid ammonia borane under high pressure. Journal of Chemical Physics, 2011, 134, 024517.	1.2	25
131	High-temperature Superconductivity in compressed Solid Silane. Scientific Reports, 2015, 5, 8845.	1.6	25
132	Uniaxial-stress-driven transformation in cold compressed glassy carbon. Applied Physics Letters, 2017, 111, .	1.5	25
133	Effect of nonhydrostatic pressure on superconductivity of monatomic iodine: An <i>ab initio</i> study. Physical Review B, 2009, 79, .	1.1	24
134	Predicted structures and superconductivity of hypothetical Mg-CH4compounds under high pressures. Materials Research Express, 2015, 2, 046001.	0.8	24
135	Intrinsic and Extrinsic Responses of ZIF-8 under High Pressure: A Combined Raman and X-ray Diffraction Investigation. Journal of Physical Chemistry C, 2019, 123, 29693-29707.	1.5	24
136	Recordâ€High Superconductivity in Transition Metal Dichalcogenides Emerged in Compressed 2Hâ€TaS ₂ . Advanced Materials, 2022, 34, e2103168.	11.1	24
137	Facile Assembly of Size- and Shape-Tunable IVâ^'VI Nanocrystals into Superlattices. Langmuir, 2010, 26, 19129-19135.	1.6	23
138	Synthesis of dendritic iridium nanostructures based on the oriented attachment mechanism and their enhanced CO and ammonia catalytic activities. Nanoscale, 2014, 6, 15059-15065.	2.8	23
139	p-Aminobenzoic acid polymorphs under high pressures. RSC Advances, 2014, 4, 15534-15541.	1.7	23
140	The low coordination number of nitrogen in hard tungsten nitrides: a first-principles study. Physical Chemistry Chemical Physics, 2015, 17, 13397-13402.	1.3	23
141	SERS Selective Enhancement on Monolayer MoS ₂ Enabled by a Pressure-Induced Shift from Resonance to Charge Transfer. ACS Applied Materials & Interfaces, 2021, 13, 26551-26560.	4.0	23
142	Effect of Rare-Earth Component of the RE/Ni Catalyst on the Formation and Nanostructure of Single-Walled Carbon Nanotubes. Journal of Physical Chemistry B, 2006, 110, 15284-15290.	1.2	22
143	Pressure-Induced Phase Transition in Guanidinium Perchlorate: A Supramolecular Structure Directed by Hydrogen Bonding and Electrostatic Interactions. Journal of Physical Chemistry B, 2011, 115, 11816-11822.	1.2	22
144	Facile synthesis of magnetic metal (Mn, Fe, Co, and Ni) oxidesnanocrystalsvia a cation-exchange reaction. Nanoscale, 2011, 3, 741-745.	2.8	22

#	Article	IF	CITATIONS
145	High-Pressure Formation of Cobalt Polyhydrides: A First-Principle Study. Inorganic Chemistry, 2018, 57, 181-186.	1.9	22
146	Structural Properties and Halogen Bonds of Cyanuric Chloride under High Pressure. Journal of Physical Chemistry B, 2011, 115, 4639-4644.	1.2	21
147	Pressure-Driven Topological Transformations of Iodine Confined in One-Dimensional Channels. Journal of Physical Chemistry C, 2013, 117, 25052-25058.	1.5	21
148	High-Pressure Studies of Abnormal Guest-Dependent Expansion in {[Cu(CO ₃) ₂](CH ₆ N ₃) ₂ } _{<i>n</i>} . Journal of Physical Chemistry C, 2014, 118, 5848-5853.	1.5	21
149	High Energetic Polymeric Nitrogen Stabilized in the Confinement of Boron Nitride Nanotube at Ambient Conditions. Journal of Physical Chemistry C, 2016, 120, 16412-16417.	1.5	21
150	Crossover from metal to insulator in dense lithium-rich compound CLi ₄ . Proceedings of the United States of America, 2016, 113, 2366-2369.	3.3	21
151	Synthesis and Electrochemical Properties of TiO ₂ â^B@C Coreâ^Shell Nanoribbons. Crystal Growth and Design, 2008, 8, 1812-1814. Pressure-induced metallization and amorphization in <mml:math< td=""><td>1.4</td><td>20</td></mml:math<>	1.4	20
152	xmlns:mml="http://www.w3.org/1998/Math/MathML"> < mml:mrow> < mml:mi mathvariant="normal">V < mml:msub> < mml:mi mathvariant="normal">O < mml:mn>2 < mml:mrow> < mml:mo> (< m	11 mi:mi) Tj I	ETQq0 0 0 rg
153	Physical Review B, 2016, 93, . Band-gap engineering and structure evolution of confined long linear carbon chains@double-walled carbon nanotubes under pressure. Carbon, 2020, 159, 266-272.	5.4	20
154	Lithium Pentazolate Synthesized by Laser Heating-Compressed Lithium Azide and Nitrogen. Journal of Physical Chemistry C, 2020, 124, 11825-11830.	1.5	20
155	Negative Volume Compressibility in Sc ₃ N@C ₈₀ –Cubane Cocrystal with Charge Transfer. Journal of the American Chemical Society, 2020, 142, 7584-7590.	6.6	20
156	Diamond-graphite nanocomposite synthesized from multi-walled carbon nanotubes fibers. Carbon, 2021, 172, 138-143.	5.4	20
157	Predicted novel metallic metastable phases of polymeric nitrogen at high pressures. New Journal of Physics, 2013, 15, 013010.	1.2	19
158	Predicted Formation of H ₃ ⁺ in Solid Halogen Polyhydrides at High Pressures. Journal of Physical Chemistry A, 2015, 119, 11059-11065.	1.1	19
159	The structural phase transition process of free-standing monoclinic vanadium dioxide micron-sized rods: temperature-dependent Raman study. RSC Advances, 2015, 5, 83139-83143.	1.7	19
160	Ground state structures of tantalum tetraboride and triboride: an ab initio study. Physical Chemistry Chemical Physics, 2016, 18, 18074-18080.	1.3	19
161	Xâ€ray diffraction of cubic Gd ₂ O ₃ /Er under high pressure. Physica Status Solidi (B): Basic Research, 2011, 248, 1123-1127.	0.7	18
162	Pressure-Induced Amorphization in Gd ₂ O ₃ /Er ³⁺ Nanorods. Journal of Physical Chemistry C, 2013, 117, 8503-8508.	1.5	18

#	Article	IF	CITATIONS
163	Pressure induced phase transition in MH2 (M = V, Nb). Journal of Chemical Physics, 2014, 140, 114703.	1.2	18
164	High-pressure close-packed structure of boron. RSC Advances, 2014, 4, 203-207.	1.7	18
165	High-Pressure-Induced Reversible Phase Transition in Sulfamide. Journal of Physical Chemistry C, 2014, 118, 18640-18645.	1.5	18
166	The effect of hydrogenation on the growth of carbon nanospheres and their performance as anode materials for rechargeable lithium-ion batteries. Nanoscale, 2015, 7, 1984-1993.	2.8	18
167	New Ordered Structure of Amorphous Carbon Clusters Induced by Fullerene–Cubane Reactions. Advanced Materials, 2018, 30, e1706916.	11.1	18
168	Pressureâ€Tailored Band Engineering for Significant Enhancements in the Photoelectric Performance of Csl ₃ in the Optical Communication Waveband. Advanced Functional Materials, 2022, 32, 2108636.	7.8	18
169	Order-disorder phase transition and dissociation of hydrogen sulfide under high pressure: <i>Ab initio</i> molecular dynamics study. Journal of Chemical Physics, 2010, 132, 164506.	1.2	17
170	Pressure-induced phase transitions of TiO ₂ nanosheets with high reactive {001} facets. RSC Advances, 2014, 4, 12873-12877.	1.7	17
171	Pressure-induced transformations of onion-like carbon nanospheres up to 48 GPa. Journal of Chemical Physics, 2015, 142, 034702.	1.2	17
172	Polymerization of Nitrogen in Ammonium Azide at High Pressures. Journal of Physical Chemistry C, 2015, 119, 25268-25272.	1.5	17
173	Confirmation of the Structural Phase Transitions in XeF ₂ under High Pressure. Journal of Physical Chemistry C, 2017, 121, 6264-6271. Effect of electrons scattered by optical phonons on superconductivity in <mml:math< td=""><td>1.5</td><td>17</td></mml:math<>	1.5	17
174	xmlns:mml="http://www.w3.org/1998/Math/MathML"> <mml:mrow><mml:mi>M</mml:mi><mml:msub><mml:m mathvariant="normal">H<mml:mn>3</mml:mn></mml:m </mml:msub></mml:mrow> () Tj ETQq0	i 0 0 rgBT / 1.1	Oyerlock 10
175	Unexpected calcium polyhydride CaH4: A possible route to dissociation of hydrogen molecules. Journal of Chemical Physics, 2019, 150, 044507.	1.2	17
176	Facile synthesis and assembly of CuS nano-flakes to novel hexagonal prism structures. Journal of Crystal Growth, 2010, 312, 2060-2064.	0.7	16
177	Investigation of stable germane structures under high-pressure. Physical Chemistry Chemical Physics, 2015, 17, 27630-27635.	1.3	16
178	High pressure and high temperature induced polymerization of doped C 60 materials. Carbon, 2016, 109, 269-275.	5.4	16
179	The elastic properties and piezochromism of polyimide films under high pressure. Polymer, 2016, 90, 1-8.	1.8	16
180	Pressure Engineering for Extending Spectral Response Range and Enhancing Photoelectric Properties of Iodine. Advanced Optical Materials, 2021, 9, 2101163.	3.6	16

#	Article	lF	CITATIONS
181	In situ Raman and photoluminescence study on pressureâ€ i nduced phase transition in C 60 nanotubes. Journal of Raman Spectroscopy, 2012, 43, 737-740.	1.2	15
182	Effect of pressure on heterocyclic compounds: Pyrimidine and s-triazine. Journal of Chemical Physics, 2014, 141, 114902.	1.2	15
183	Hydrogen Bond in Compressed Solid Hydrazine. Journal of Physical Chemistry C, 2014, 118, 3236-3243.	1.5	15
184	Pressure-Induced Phase Transition in Hydrogen-Bonded Supramolecular Structure: Ammonium Formate. Journal of Physical Chemistry C, 2014, 118, 8521-8530.	1.5	15
185	Prediction of stoichiometric PoHn compounds: crystal structures and properties. RSC Advances, 2015, 5, 103445-103450.	1.7	15
186	Enhancement of Tc in the atomic phase of iodine-doped hydrogen at high pressures. Physical Chemistry Chemical Physics, 2015, 17, 32335-32340.	1.3	15
187	Discovery of High-Pressure Polymorphs for a Typical Polymorphic System: Oxalyl Dihydrazide. Journal of Physical Chemistry C, 2015, 119, 10178-10188.	1.5	15
188	Polarized Raman Study of Aligned Multiwalled Carbon Nanotubes Arrays under High Pressure. Journal of Physical Chemistry C, 2015, 119, 27759-27767.	1.5	15
189	Pressure induced metastable polymerization in doped C60 materials. Carbon, 2017, 115, 740-745.	5.4	15
190	Photoluminescence properties of high-pressure-polymerized C60 nanorods in the orthorhombic and tetragonal phases. Applied Physics Letters, 2006, 89, 181925.	1.5	14
191	Mutual Transformation between Random Nanoparticles and Their Superlattices: The Configuration of Capping Ligand Chains. Journal of Physical Chemistry C, 2010, 114, 11425-11429.	1.5	14
192	High pressure and high temperature induced polymerization of C60 nanotubes. CrystEngComm, 2011, 13, 3600.	1.3	14
193	The structural stability of AlPO4-5 zeolite under pressure: Effect of the pressure transmission medium. Journal of Applied Physics, 2012, 111, .	1.1	14
194	High pressure behaviors of nanoporous anatase TiO2. Materials Research Bulletin, 2012, 47, 1396-1399.	2.7	14
195	Shape-controlled synthesis of PbS nanostructures from â^'20 to 240 °C: the competitive process between growth kinetics and thermodynamics. CrystEngComm, 2013, 15, 5496.	1.3	14
196	Structural transformation of confined iodine in the elliptical channels of AlPO4-11 crystals under high pressure. Physical Chemistry Chemical Physics, 2014, 16, 8301.	1.3	14
197	Structural, mechanical and electronic properties of Rh2B and RhB2: first-principles calculations. Scientific Reports, 2015, 5, 10500.	1.6	14
198	Strong covalent boron bonding induced extreme hardness of VB3. Journal of Alloys and Compounds, 2016, 688, 1101-1107.	2.8	14

#	Article	IF	CITATIONS
199	Nanosize effects assisted synthesis of the high pressure metastable phase in ZrO2. Nanoscale, 2016, 8, 2412-2417.	2.8	14
200	Morphology-Tuned Phase Transitions of Horseshoe Shaped BaTiO ₃ Nanomaterials under High Pressure. Journal of Physical Chemistry C, 2018, 122, 5188-5194.	1.5	14
201	High energetic polymeric nitrogen sheet confined in a graphene matrix. RSC Advances, 2018, 8, 30912-30918.	1.7	14
202	Pressure-induced polymerization of nano- and submicrometer C60 rods into a rhombohedral phase. Chemical Physics Letters, 2006, 423, 215-219.	1.2	13
203	High pressure and high temperature induced polymeric C60 nanocrystal. Diamond and Related Materials, 2008, 17, 620-623.	1.8	13
204	Compression and Probing Câ^'H···I Hydrogen Bonds of Iodoform under High Pressure by X-ray Diffraction and Raman Scattering. Journal of Physical Chemistry B, 2009, 113, 7430-7434.	1.2	13
205	Reversible pressure-induced polymerization of Fe(C5H5)2 doped C70. Carbon, 2013, 62, 447-454.	5.4	13
206	Structural stability and compressive behavior of ZrH ₂ under hydrostatic pressure and nonhydrostatic pressure. RSC Advances, 2014, 4, 46780-46786.	1.7	13
207	Pressure-Induced Diversity of π-Stacking Motifs and Amorphous Polymerization in Pyrrole. Journal of Physical Chemistry C, 2014, 118, 12420-12427.	1.5	13
208	Ab initio investigation of CaO-ZnO alloys under high pressure. Scientific Reports, 2015, 5, 11003.	1.6	13
209	Ab initio structure determination of n-diamond. Scientific Reports, 2015, 5, 13447.	1.6	13
210	High pressure synthesis of amorphous TiO2 nanotubes. AIP Advances, 2015, 5, 097128.	0.6	13
211	Ab initio study of germanium-hydride compounds under high pressure. RSC Advances, 2015, 5, 19432-19438.	1.7	13
212	High-pressure Raman study of solid hydrogen up to 300 GPa. Chinese Physics B, 2016, 25, 037401.	0.7	13
213	The pressure-induced metallization of monoclinic vanadium dioxide. RSC Advances, 2016, 6, 104949-104954.	1.7	13
214	Structural stability and electronic property in K ₂ S under pressure. RSC Advances, 2017, 7, 7424-7430.	1.7	13
215	Two-dimensional carbon dioxide with high stability, a negative Poisson's ratio and a huge band gap. Physical Chemistry Chemical Physics, 2018, 20, 20615-20621.	1.3	13
216	Cobalt–Nitrogen Compounds at High Pressure. Inorganic Chemistry, 2021, 60, 14022-14030.	1.9	13

#	Article	IF	CITATIONS
217	Structural and Electronic Changes of SnBr ₄ under High Pressure. Journal of Physical Chemistry C, 2013, 117, 8381-8387.	1.5	12
218	Pure Hexagonal Phase of EuF ₃ Modulated by High Pressure. Journal of Physical Chemistry C, 2014, 118, 7562-7568.	1.5	12
219	Insertion of N2 into the Channels of AFI Zeolite under High Pressure. Scientific Reports, 2015, 5, 13234.	1.6	12
220	Manganese oxide nanostructures: low-temperature selective synthesis and thermal conversion. RSC Advances, 2015, 5, 25250-25257.	1.7	12
221	High pressure studies of trimethyltin azide by Raman scattering, IR absorption, and synchrotron X-ray diffraction. RSC Advances, 2016, 6, 98921-98926.	1.7	12
222	High-Pressure Studies of 4-Acetamidobenzenesulfonyl Azide: Combined Raman Scattering, IR Absorption, and Synchrotron X-ray Diffraction Measurements. Journal of Physical Chemistry B, 2016, 120, 12015-12022.	1.2	12
223	<i>Gauche</i> – <i>trans</i> Conformational Equilibrium of Succinonitrile under High Pressure. Journal of Physical Chemistry C, 2016, 120, 5340-5346.	1.5	12
224	A Novel High-Density Phase and Amorphization of Nitrogen-Rich 1H-Tetrazole (CH2N4) under High Pressure. Scientific Reports, 2017, 7, 39249.	1.6	12
225	Pressure-induced phase transitions and insulator-metal transitions in VO2 nanoparticles. Journal of Alloys and Compounds, 2017, 709, 260-266.	2.8	12
226	Semiconductor-to-metal transition in HfSe2 under high pressure. Journal of Alloys and Compounds, 2021, 867, 158923.	2.8	12
227	Compression studies of face-to-face <i>Ï€</i> -stacking interaction in sodium squarate salts: Na2C4O4 and Na2C4O4•3H2O. Journal of Chemical Physics, 2012, 137, 184905.	1.2	11
228	A facile method to synthesize nanosized metal oxides from their corresponding bulk materials. CrystEngComm, 2012, 14, 5937.	1.3	11
229	ZnS nanocrystals and nanoflowers synthesized by a green chemistry approach: Rare excitonic photoluminescence achieved by the tunable molar ratio of precursors. Journal of Hazardous Materials, 2012, 211-212, 62-67.	6.5	11
230	High pressure supramolecular chemistry. Science Bulletin, 2014, 59, 5258-5268.	1.7	11
231	Experimental verification of the high pressure crystal structures in NH3BH3. Journal of Chemical Physics, 2014, 140, 244507.	1.2	11
232	Synthesis of SnO nanocrystals with shape control via ligands interaction and limited ligand protection. Colloids and Surfaces A: Physicochemical and Engineering Aspects, 2010, 363, 30-34.	2.3	10
233	The crystal structure and superconducting properties of monatomic bromine. Journal of Physics Condensed Matter, 2010, 22, 015702.	0.7	10
234	Shape and crystal phase controlled synthesis of InSe nanocrystals via a simple and facile way. Journal of Crystal Growth, 2011, 336, 1-5.	0.7	10

#	Article	IF	CITATIONS
235	High-Pressure Stability and Compressibility of Zircon-Type YV _{1–<i>x</i>} P _{<i>x</i>} O ₄ :Eu ³⁺ Solid-Solution Nanoparticles: An X-ray Diffraction and Raman Spectroscopy Study. Journal of Physical Chemistry C, 2013, 117, 18603-18612.	1.5	10
236	Exploring the possible interlinked structures in singleâ€wall carbon nanotubes under pressure by Raman spectroscopy. Journal of Raman Spectroscopy, 2013, 44, 176-182.	1.2	10
237	The crystal structure of IrB ₂ : a first-principle calculation. RSC Advances, 2014, 4, 63442-63446.	1.7	10
238	The control of the morphologies, structures and photoluminescence properties of C70 nano/microcrystals with different trichlorobenzene isomers. CrystEngComm, 2014, 16, 3284.	1.3	10
239	New Assembly of Acetamidinium Nitrate Modulated by High Pressure. Journal of Physical Chemistry C, 2014, 118, 23443-23450.	1.5	10
240	Analysis of the upconversion photoluminescence spectra as a probe of local microstructure in Y ₂ O ₃ /Eu ³⁺ nanotubes under high pressure. RSC Advances, 2015, 5, 3130-3134.	1.7	10
241	Pressure-induced transformations in carbon nano-onions. Journal of Applied Physics, 2016, 119, .	1.1	10
242	Photoluminescence changes of C70 nano/submicro-crystals induced by high pressure and high temperature. Scientific Reports, 2016, 6, 38470.	1.6	10
243	Pressure-induced phase transition of SnH ₄ : a new layered structure. RSC Advances, 2016, 6, 10456-10461.	1.7	10
244	Unravelling decomposition products of phosphine under high pressure. Journal of Raman Spectroscopy, 2018, 49, 721-727.	1.2	10
245	Graphdiyne under pressure: A Raman study. Applied Physics Letters, 2018, 113, .	1.5	10
246	How to get superhard MnB2: a first-principles study. Journal of Materials Chemistry, 2012, 22, 17630.	6.7	9
247	Pressure-induced amorphization in orthorhombic Ta2O5: An intrinsic character of crystal. Journal of Applied Physics, 2014, 115, .	1.1	9
248	Raman spectroscopy of bromine chains inside the one-dimensional channels of AlPO ₄ -5 single crystals. Journal of Raman Spectroscopy, 2015, 46, 413-417.	1.2	9
249	A novel stable hydrogen-rich SnH8 under high pressure. RSC Advances, 2015, 5, 107637-107641.	1.7	9
250	Ab initio study of native point defects in ZnO under pressure. Solid State Communications, 2015, 201, 130-134.	0.9	9
251	Phase Transition for Zinc Sulfide Nanosheets under High Pressure. Journal of Physical Chemistry C, 2016, 120, 781-785.	1.5	9
252	Revealing unusual rigid diamond net analogues in superhard titanium carbides. RSC Advances, 2018, 8, 14479-14487.	1.7	9

#	Article	IF	CITATIONS
253	Direct Conversion of Graphene Aerogel into Low-Density Diamond Aerogel Composed of Ultrasmall Nanocrystals. Journal of Physical Chemistry C, 2018, 122, 13193-13198.	1.5	9
254	Nonstoichiometric amorphous silicon carbide films as promising antireflection and protective coatings for germanium in IR spectral range. Optical Materials, 2019, 88, 445-450.	1.7	9
255	Size and morphology effects on the high pressure behaviors of Mn ₃ O ₄ nanorods. Nanoscale Advances, 2020, 2, 5841-5847.	2.2	9
256	Raman study of bromine-doped single-walled carbon nanotubes under high pressure. Journal of Physics Condensed Matter, 2002, 14, 11255-11259.	0.7	8
257	Resistivity and fractal structure in carbon nanotube networks. Journal of Physics Condensed Matter, 2002, 14, 11125-11129.	0.7	8
258	Pressure-induced magnetic transition in metallic nickel hydrides byab initiopseudopotential plane-wave calculations. Physical Review B, 2006, 74, .	1.1	8
259	Synchrotron X-ray Diffraction and Infrared Spectroscopy Studies of C ₆₀ H ₁₈ under High Pressure. Journal of Physical Chemistry Letters, 2010, 1, 714-719.	2.1	8
260	The hydrogenâ€bond effect on the high pressure behavior of hydrazinium monochloride. Journal of Raman Spectroscopy, 2015, 46, 266-272.	1.2	8
261	Polymeric Nitrogen A7 Layers Stabilized in the Confinement of a Multilayer BN Matrix at Ambient Conditions. Scientific Reports, 2018, 8, 13758.	1.6	8
262	Pressure-stabilized polymerization of nitrogen in manganese nitrides at ambient and high pressures. Physical Chemistry Chemical Physics, 2022, 24, 5738-5747.	1.3	8
263	Significant pressure-induced enhancement of photoelectric properties of WS ₂ in the near-infrared region. Materials Research Letters, 2022, 10, 547-555.	4.1	8
264	A New High-Pressure Polar Phase of Crystalline Bromoform: A First-Principles Study. Journal of Physical Chemistry B, 2010, 114, 13933-13939.	1.2	7
265	Application of a new composite cubic-boron nitride gasket assembly for high pressure inelastic x-ray scattering studies of carbon related materials. Review of Scientific Instruments, 2011, 82, 073902.	0.6	7
266	Synthesis of TiO ₂ @C core–shell nanostructures with various crystal structures by hydrothermal and postheat treatments. Journal of Materials Research, 2013, 28, 449-453.	1.2	7
267	Structural Deformation of Sm@C88 under High Pressure. Scientific Reports, 2015, 5, 13398.	1.6	7
268	High-pressure behavior of bromine confined in the one-dimensional channels of zeolite AlPO4-5 single crystals. Journal of Chemical Physics, 2016, 145, 124319.	1.2	7
269	In situ low-temperature Raman studies of iodine molecules confined in the one-dimensional channels of AIPO 4 -5 crystals. Microporous and Mesoporous Materials, 2016, 221, 76-80.	2.2	7
270	Remarkable cycle-activated capacity increasing in onion-like carbon nanospheres as lithium battery anode material. Nanotechnology, 2017, 28, 035704.	1.3	7

#	Article	IF	CITATIONS
271	Effect of C ₇₀ rotation on the photoluminescence spectra of compressed C ₇₀ *mesitylene. Journal of Raman Spectroscopy, 2017, 48, 437-442.	1.2	7
272	A high pressure Raman study on confined individual iodine molecules as molecular probes of structural collapse in the AlPO ₄ -5 framework. Physical Chemistry Chemical Physics, 2018, 20, 26117-26125.	1.3	7
273	Vibrational Properties and Polymerization of Corannulene under Pressure, Probed by Raman and Infrared Spectroscopies. Journal of Physical Chemistry C, 2019, 123, 23674-23681.	1.5	7
274	High temperature driven transformation of iodine species in AFI and AEL channels: A comparative study. Microporous and Mesoporous Materials, 2019, 290, 109682.	2.2	7
275	Pressure induced transformation and subsequent amorphization of monoclinic Nb ₂ O ₅ and its effect on optical properties. Journal of Physics Condensed Matter, 2019, 31, 105401.	0.7	7
276	Effects of pressure on the structure and properties of layered ferromagnetic Cr2Ge2Te6. Physica B: Condensed Matter, 2020, 595, 412344.	1.3	7
277	Structural, electronic, and optical properties of crystalline iodoform under high pressure: A first-principles study. Journal of Chemical Physics, 2011, 134, 034508.	1.2	6
278	Buckminsterfullerene: A Strong, Covalently Bonded, Reinforcing Filler and Reversible Cross-Linker in the Form of Clusters in a Polymer. ACS Macro Letters, 2013, 2, 511-517.	2.3	6
279	High-pressure phase transition of MH3 (M: Er, Ho). Journal of Chemical Physics, 2014, 141, 054703.	1.2	6
280	Effects of hydrothermal conditions on the morphology and phase composition of synthesized TiO2 nanostructures. Physica B: Condensed Matter, 2014, 445, 42-47.	1.3	6
281	Transformations of iodine species inside elliptical channels of AlPO ₄ -11 crystals at low temperature: a Raman study. Journal of Raman Spectroscopy, 2015, 46, 400-405.	1.2	6
282	Pressure-Induced Phase Transitions and Amorphization of 4-Carboxybenzenesulfonyl Azide. Journal of Physical Chemistry C, 2016, 120, 25709-25716.	1.5	6
283	First-principles study of ternary Li-Al-Te compounds under high pressure. Solid State Communications, 2018, 270, 58-64.	0.9	6
284	Structural and electrical properties of Ga–Te systems under high pressure. Chinese Physics B, 2019, 28, 056104.	0.7	6
285	Crystallized phosphorus/carbon composites with tunable P C bonds by high pressure and high temperature. Journal of Physics and Chemistry of Solids, 2019, 130, 250-255.	1.9	6
286	Versatile GalnO ₃ -sheet with strain-tunable electronic structure, excellent mechanical flexibility, and an ideal gap for photovoltaics. Chinese Physics B, 2019, 28, 016105.	0.7	6
287	First principle studies of ZnO1-xSx alloys under high pressure. Journal of Alloys and Compounds, 2019, 788, 905-911.	2.8	6
288	Preparation and pressure-induced semiconductor-metal transition of CrSi2 nanocrystals. Materials Letters, 1999, 41, 97-100.	1.3	5

#	Article	IF	CITATIONS
289	The structure and dynamics analysis of one-dimension confined C3V symmetrical C60H18 molecules in single-wall carbon nanotube. CrystEngComm, 2013, 15, 7723.	1.3	5
290	The pressure induced amorphization and behavior of octahedron in Y ₂ O ₃ /Eu ³⁺ nanotubes. Materials Research Express, 2014, 1, 025013.	0.8	5
291	Pressure-Induced Amorphization and Recrystallization of SnI ₂ . Journal of Physical Chemistry C, 2015, 119, 19312-19317.	1.5	5
292	Pressure-induced structural transformation of CaC2. Journal of Chemical Physics, 2016, 144, 194506.	1.2	5
293	Ab initio molecular dynamic study of solid-state transitions of ammonium nitrate. Scientific Reports, 2016, 6, 18918.	1.6	5
294	Structural Stability and Deformation of Solvated Sm@C2(42)-C90 under High Pressure. Scientific Reports, 2016, 6, 31213.	1.6	5
295	High pressure studies of Ni ₃ [(C ₂ H ₅ N ₅) ₆ (H ₂ O) _{6by Raman scattering, IR absorption, and synchrotron X-ray diffraction. RSC Advances, 2016, 6, 65031-65037.}	0>](NO <si 1.7</si 	ub>3
296	High pressure infrared spectroscopy study on C60â^—CS2 solvates. Chemical Physics Letters, 2017, 669, 49-53.	1.2	5
297	Investigation of the polymerization mechanism of ferrocene doped C60 under high pressure and high temperature. Scientific Reports, 2017, 7, 10809.	1.6	5
298	Unexpected stable stoichiometries and superconductivity of potassium-rich sulfides. RSC Advances, 2017, 7, 44884-44889.	1.7	5
299	Optical properties and structural phase transitions of W-doped VO2(R) under pressure. RSC Advances, 2017, 7, 31597-31602.	1.7	5
300	Emergent property of high hardness for C-rich ruthenium carbides: partial covalent Ru–Ru bonds. Physical Chemistry Chemical Physics, 2018, 20, 6108-6115.	1.3	5
301	Structural model of substitutional sulfur in diamond*. Chinese Physics B, 2019, 28, 088102.	0.7	5
302	Crystal structures and decomposing of B–P compounds under pressure*. Chinese Physics B, 2019, 28, 056101.	0.7	5
303	Evolution of hydrogen dissolution and superconductivity in Re-based solid solutions under pressure studied by <i>ab initio</i> calculations. Physical Review B, 2021, 103, .	1.1	5
304	Size and Shape's Effects on the High-Pressure Behavior of WS2 Nanomaterials. Materials, 2022, 15, 2838.	1.3	5
305	The New High-Pressure Phases of Nitrogen-Rich Ag–N Compounds. Materials, 2022, 15, 4986.	1.3	5
306	High pressure superconducting phase of BI3: an ab initio study. RSC Advances, 2014, 4, 32068-32074.	1.7	4

#	Article	IF	CITATIONS
307	High-pressure polymorphism as a step towards high density structures of LiAlH4. Applied Physics Letters, 2015, 107, 041906.	1.5	4
308	Optoelectronic investigation of corundum Mg4Nb2O9 single crystal. Journal of Alloys and Compounds, 2015, 619, 240-243.	2.8	4
309	Unexpected photoluminescence properties from one-dimensional molecular chains. Nanoscale, 2016, 8, 1456-1461.	2.8	4
310	Raman study of graphene nanoribbon analogs confined in singleâ€walled carbon nanotubes and their highâ€pressure transformations. Journal of Raman Spectroscopy, 2017, 48, 951-957.	1.2	4
311	Insights into Antibonding Induced Energy Density Enhancement and Exotic Electronic Properties for Germanium Nitrides at Modest Pressures. Inorganic Chemistry, 2018, 57, 10416-10423.	1.9	4
312	Pressure-Induced Reversible Phase Transitions in a New Metastable Phase of Vanadium Dioxide. Journal of Physical Chemistry C, 2019, 123, 955-962.	1.5	4
313	Evolution of metallization and superconductivity in solid hydrogen. Physics Letters, Section A: General, Atomic and Solid State Physics, 2020, 384, 126571.	0.9	4
314	Comparative study of pressure-induced polymerization in C ₆₀ nanorods and single crystals. Journal of Physics Condensed Matter, 2007, 19, 425207.	0.7	3
315	Synthesis and solid-state studies of self-assembled C60 microtubes. Diamond and Related Materials, 2011, 20, 178-182.	1.8	3
316	Effects of alcohols on shape-tuning and luminescence-enhancing of C70 nanocrystals. Optical Materials, 2013, 36, 449-454.	1.7	3
317	Preferable orientation of spherical fullerene inside boron nitride nanotubes. Journal of Physics Condensed Matter, 2013, 25, 065402.	0.7	3
318	Structure determination of ultra dense magnesium borohydride: A first-principles study. Journal of Chemical Physics, 2013, 138, 214503.	1.2	3
319	Optical floating zone method growth and optical properties of corundum Mg4Nb2O9 single crystal. Journal of Crystal Growth, 2014, 402, 109-112.	0.7	3
320	Ab initio study on the stability of N-doped ZnO under high pressure. RSC Advances, 2015, 5, 16774-16779.	1.7	3
321	Investigation of the lattice behavior of cubic Y ₂ O ₃ /Eu ³⁺ nanotubes under high pressure. Physica Status Solidi (B): Basic Research, 2016, 253, 2204-2208.	0.7	3
322	One-step synthesis of C60 nano-assemblies at different temperatures. Materials and Design, 2016, 93, 343-346.	3.3	3
323	High-pressure structures of helium and carbon dioxide from first-principles calculations. Solid State Communications, 2018, 283, 9-13.	0.9	3
324	Structural, Electronic, and Optical Properties of ZnO _{1 – <i>x</i>} Te _{<i>x</i>} Alloys. Physica Status Solidi - Rapid Research Letters, 2019, 13, 1900155.	1.2	3

#	Article	IF	CITATIONS
325	High-pressure new phase of AgN ₃ . Modern Physics Letters B, 2021, 35, 2150386.	1.0	3
326	High Pressure and High Temperature Induced Polymerization of C ₆₀ Solvates: The Effect of Intercalated Aromatic Solvents. Journal of Physical Chemistry C, 2021, 125, 17155-17163.	1.5	3
327	Improvement of radiation stability of semi-insulating gallium arsenide crystals by deposition of diamond-like carbon films. Optical Materials, 2016, 62, 372-377.	1.7	2
328	Elastic properties of single crystal hydrogen sulfide: A Brillouin scattering study under high pressure-temperature. Journal of Applied Physics, 2018, 124, 125901.	1.1	2
329	Study on disordered graphitic nanocarbon under pressure and their transformation into polycrystalline nanodiamond. Chemical Physics Letters, 2019, 730, 491-496.	1.2	2
330	The hardness mechanism and bonding properties of CrN2: A first principle study. Computational Materials Science, 2019, 158, 282-288.	1.4	2
331	Pressureâ€induced insertion and transformation of N ₂ in the cavities of zeolitic imidazolate frameworkâ€8: A Raman study. Journal of Raman Spectroscopy, 2020, 51, 1230-1239.	1.2	2
332	Anomalous phonon softening of G-band in compressed graphitic carbon nitride due to strong electrostatic repulsion. Applied Physics Letters, 2021, 118, .	1.5	2
333	Pressure-Induced Electronic and Structural Transition in Nodal-Line Semimetal ZrSiSe. Inorganic Chemistry, 2021, 60, 11140-11146.	1.9	2
334	An investigation of the effect of high-pressure on charge transfer in dye-sensitized solar cells based on surface-enhanced Raman spectroscopy. Nanoscale, 2022, 14, 373-381.	2.8	2
335	Structural Evolution of D _{5h} (1)-C ₉₀ under High Pressure: A Mediate Allotrope of Nanocarbon from Zero-Dimensional Fullerene to One-Dimensional Nanotube. Chinese Physics Letters, 2022, 39, 056101.	1.3	2
336	High-Pressure Synthesis and Stability Enhancement of Lithium Pentazolate. Inorganic Chemistry, 2022, 61, 9012-9018.	1.9	2
337	Decoration of C60 nanorods with nickel and their magnetic properties. Science Bulletin, 2009, 54, 2539-2542.	1.7	1
338	Stable structures and superconductivity of an At–H system at high pressure. Physical Chemistry Chemical Physics, 2018, 20, 24783-24789.	1.3	1
339	Synthesis and high pressure studies of white luminescence host–guest complex nanocrystals based on C60 and p-But-calix[8]arene. Nanotechnology, 2020, 31, 165701.	1.3	1
340	Realization of pressure induced emission enhancement for rare earth luminescent materials: Adopting delta-doped structure. Journal of Alloys and Compounds, 2021, 859, 157882.	2.8	1
341	Bromine Doped Single-walled Carbon Nanotubes. Materials Research Society Symposia Proceedings, 2000, 633, 13361.	0.1	0
342	High Pressure and High Temperature Induced Polymeric C60 Nanorods and Their Photoluminescence Properties. Materials Research Society Symposia Proceedings, 2006, 987, 1.	0.1	0

#	Article	IF	CITATIONS
343	High pressure structural stability of the Na-Te system. AIP Advances, 2018, 8, 035123.	0.6	0
344	A first-principles study on crystal structures and metallization of sodium-rich sulfides under high pressure. Journal of Physics Condensed Matter, 2022, , .	0.7	0